

ARTICLE TYPE**Tracking Control by the Newton-Raphson Method with Output Prediction and Controller Speedup[†]**Y. Wardi*¹ | C. Seatzu² | J. Cortés³ | M. Egerstedt⁴ | S. Shivam¹ | I. Buckley⁵¹School of Electrical and Computer Engineering, Georgia Institute of Technology, Atlanta, USA²Department of Electrical and Electronic Engineering, University of Cagliari, Italy³Department of Mechanical and Aerospace Engineering, University of California, San Diego, USA⁴Samueli School of Engineering, University of California, Irvine, USA⁵Agtonomy, San Francisco, California, USA**Correspondence***Yorai Wardi, School of Electrical and Computer Engineering, Georgia Institute of Technology, Atlanta, GA 30332, USA.
Email: ywardi@ece.gatech.edu**Summary**

This paper presents a control technique for output tracking of reference signals in continuous-time dynamical systems. The technique is comprised of the following three elements: (i) a fluid-flow version of the Newton-Raphson method for solving algebraic equations, (ii) a system-output prediction which has to track the future reference signal, and (iii) a speedup of the control action for enhancing the tracker's accuracy and, in some cases, stabilizing the closed-loop system. The technique can be suitable for linear and nonlinear systems, implementable by simple algorithms, and can track reference points as well as time-dependent reference signals. Though inherently local, the tracking controller is proven to have a global convergence for a class of linear systems. The derived theoretical results of the paper include convergence of the tracking controller and error analysis, and are supported by illustrative simulation and laboratory experiments.

KEYWORDS:

Nonlinear tracking, Newton-Raphson flow, controller speedup, output prediction

1 | INTRODUCTION

The subject of this paper is a reference-tracking control technique for dynamical systems modelled by ordinary differential equations. The technique is founded on real-time implementations of a fluid-flow variant of the Newton-Raphson method for solving algebraic equations. The relevance of the Newton-Raphson method is due to the observation, argued for in the sequel, that tracking can be viewed as a dynamic process of attempting to solve a time-dependent suite of nonlinear algebraic equations.

Existing nonlinear regulation techniques such as the Byrnes-Isidori regulator [1], Khalil's high-gain observers for output regulation [2], and Model Predictive Control (MPC) [3] are more general and perhaps more powerful than the technique presented here. However, their effectiveness is partly due to significant computational sophistication like nonlinear inversions, the appropriate nonlinear normal form, or real-time algorithms for optimal control. The control technique described in this paper, defined by a dynamic-feedback law, is simple and requires low computing efforts. It has some elements of MPC, but also intrinsic differences from it which will be highlighted in the sequel. It is not based on linearization, but rather on a differential equation which may be nonlinear. Having its foundations in the Newton-Raphson flow it is essentially a local method, but may have a fast convergence. Also, in some cases it may be globally convergent. This will be proved for linear systems, while simulations will demonstrate the efficacy of the controller on various examples of nonlinear systems.

[†]Seatzu's work is supported by the Region of Sardinia Project RASSR05871 MOSIMA, FSC 2014-2020, Annuity 2017, Subject Area 3, Action Line 3.1.

Cortés' work is supported by NSF Award CNS-1446891.

Egerstedt's work is supported by grant DCIST CRA W911NF-17-2-0181 from the US Army Research Lab.

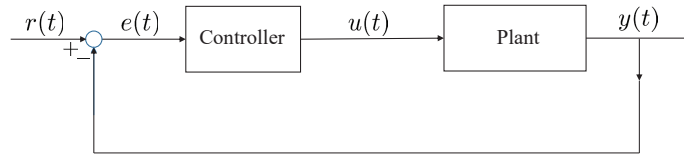


FIGURE 1 Basic control system

The system-diagram that we consider is depicted in Figure 1, where the reference signal $r(t)$, control input $u(t)$, and system output $y(t)$ are all in \mathcal{R}^m for a given $m \in \{1, 2, \dots\}$. The condition that the reference, control, and output have the same dimension is essential for the present discussion, and although ad-hoc ways to circumvent the effects of its absence have begun to emerge [4], we defer their general exposition to a future publication.

The plant subsystem in Figure 1 is a dynamical system based on an ordinary differential equation, whose input, state, and output variables are denoted by $u(t) \in \mathcal{R}^m$, $x(t) \in \mathcal{R}^n$ for some $n \in \{1, 2, \dots\}$, and $y(t) \in \mathcal{R}^m$, respectively. Given a fixed prediction horizon $T > 0$, let $\hat{y}(t+T)$ denote a predicted value of $y(t+T)$. The tracking technique, implemented by the controller, is underscored by a process aiming at solving the time (t)-dependent equation $r(t+T) - \hat{y}(t+T) = 0$.¹ The predictor $\hat{y}(t+T)$ is assumed to be a function of $x(t)$ and $u(t)$, and correspondingly, the tracking controller defines the time-derivative $\dot{u}(t)$ by a differential equation in terms of $(x(t), u(t))$ as well. Under the ideal condition of perfect output prediction, this feedback law can result in perfect asymptotic tracking under suitable assumptions. In the presence of prediction errors, the asymptotic tracking error will be shown to be equal to the asymptotic prediction error. Furthermore, it will be proved that an increase in the controller's rate (defined below) can stabilize the closed-loop system and reduce tracking errors that are due to certain disturbances and computational errors in the loop. All of this will be defined and described in detail in the later sections.

To explain the term “fluid-flow variant” of an iterative algorithm in \mathcal{R}^m , and place the forthcoming results in the context of the established literature, consider an algorithm of the form

$$u_{k+1} = u_k + g(u_k), \quad (1)$$

$k = 0, 1, \dots$, where $u_k \in \mathcal{R}^m$, and $g : \mathcal{R}^m \rightarrow \mathcal{R}^m$ is a function assumed to be locally Lipschitz continuous. Placing the algorithm in a temporal framework, suppose that an iteration according to (1) is computed once every Δt seconds for a given $\Delta t > 0$, and scale the step size in the Right-Hand Side (RHS) of (1) by Δt . Defining $u(k\Delta t) := u_k$ and taking the limit $\Delta t \rightarrow 0$ we obtain the following equation,

$$\dot{u}(t) = g(u(t)). \quad (2)$$

The process defined by Eq. (2) is said to be the *fluid-flow version of the algorithm* defined by Eq. (1). Fluid-flow processes can be useful in investigating asymptotic properties of their associated discrete algorithms with small step sizes, such as convergence and rate of convergence, optimality and stability of limit points, etc. They have been applied mainly to the design of gradient-descent algorithms for problems in optimization and linear algebra, including sorting, eigenvalue decomposition, and linear programming; see [5, 6, 7] for early works. Ref. [6] recognized their potential applications in massively-parallel computing platforms such as neural nets, slated to solve very-large scale problems. Recent applications to learning and distributed optimization can be found in [8] and [9], respectively, and references therein.

Fluid-flow variants of the Newton-Raphson method have been considered as well due to their superlinear convergence rates. Refs. [10, 11] consider first- and second-order algorithms for convex (or concave) constrained programs with time-varying cost functions. Ref. [10] is concerned with applications to traffic engineering in telecommunication networks, and Ref. [11] considers distributed optimization over multi-agent networks with consensus constraints. Both references derive general theoretical results in abstract settings of the Newton-Raphson flow beyond their motivating problem-classes, including convergence under weak smoothness assumptions and convergence in a general network setting, respectively. Ref. [12] derives a continuous-flow, primal-dual technique for convex optimization without assuming differentiability of the cost function. Combining results from the theory of convex, nondifferentiable optimization with fluid-flow techniques, it defines the flow by differential inclusions, and

¹ $r(t+T)$ refers to the target point of tracking by $\hat{y}(t+T)$. We do not specify how it is defined or computed; it includes situations where $r(t+T)$ is a future point of an exogenous process or a predicted value of an endogenous process. More about that will be said in the sequel.

derives convergence results, including global asymptotic stability of the minimum and superlinear/quadratic (depending on the assumptions) convergence under the weakest-to-date smoothness assumptions on the cost function.

This paper applies a fluid-flow variant of the Newton-Raphson method to finding roots of algebraic equations rather than optimization. In contrast to the aforementioned references, the resulting control-derivative $\dot{u}(t)$ cannot be defined or described by an equation like (2). However, it can be defined in terms of a predicted output $\hat{y}(t+T)$, which in turn is taken to be a function of $(x(t), u(t))$. This is the reason we use an output predictor to define the tracking controller.

Regarding the third element of the proposed technique mentioned in the Abstract, the idea that a high controller's rate can enhance stability-robustness and speed up tracking-convergence is implicit in [13] and explicit in [14]. This paper, as mentioned, explores it in conjunction with the Newton-Raphson flow and output prediction, in the aforementioned setting of tracking-control.

The rest of the paper is structured as follows. Section 2 presents the problem and recounts the past developments of our tracking-control technique. Section 3 carries out analyses of tracking-convergence and how it is impacted by disturbances and other errors in the loop. Section 4 derives a verifiable sufficient condition for stability of linear systems at high controller rates. Section 5 presents simulation results and Section 6 describes a laboratory experiment. Finally, Section 7 concludes the paper.

Preliminary results concerning the material in this paper can be found in the following four conference papers, [15, 16, 17, 4]. This paper extends them in the following ways: 1). It presents a new version of the controller which can yield perfect asymptotic tracking, in contrast with the above-mentioned references where only approximate tracking is obtained. 2). Its main results, concerning asymptotic convergence and error analysis in a general setting, and contained in Sections 3 and 4, are new. 3). The simulation and laboratory examples, contained in Sections 5 and 6, are new.

An *arxiv* version of the paper [18] contains some expanded discussions as well as straightforward proofs of lemmas which are stated but unproved in the sequel.

2 | PROBLEM FORMULATION AND EARLIER RESULTS

This section provides a background material on the specific problem considered in the paper, including its early formulation and the fundamental approach to it taken by the authors. Much of the surveyed material can be found in [15].

Consider first the simple case where the plant system in Figure 1 is a memoryless nonlinearity of the form

$$y(t) = g(u(t)), \quad (3)$$

where the function $g : \mathcal{R}^m \rightarrow \mathcal{R}^m$ is continuously differentiable. The tracking problem can be viewed as an attempt to solve the time-dependent system of equations

$$r(t) - g(u) = 0 \quad (4)$$

in the variable $u \in \mathcal{R}^m$, and the controller has to be designed to ensure that

$$\lim_{t \rightarrow \infty} (r(t) - g(u(t))) = 0. \quad (5)$$

To solve this problem we define the controller subsystem in Figure 1 so as to implement the fluid-flow version of the Newton-Raphson method. It has the following form,

$$\dot{u}(t) = \left(\frac{\partial g}{\partial u}(u(t)) \right)^{-1} (r(t) - g(u(t))), \quad (6)$$

assuming that the Jacobian $\frac{\partial g}{\partial u}(u(t))$ is nonsingular for all $t \geq 0$. This assumption suggests that the tracking controller cannot be expected to have a global convergence but only a local domain of attraction, which is a common feature of the Newton-Raphson method.

To illustrate the argument underscoring the local tracking of the controller defined by Eq. (6), suppose for a moment that $r(t) \equiv r \in \mathcal{R}^m$, a constant reference assumed to lie in the range of the function $g(\cdot)$. Fix $\hat{u} \in \mathcal{R}^m$ such that $g(\hat{u}) = r$, and suppose that $\frac{\partial g}{\partial u}(\hat{u})$ is nonsingular. Let $\Omega \subset \mathcal{R}^m$ be an open set containing \hat{u} such that its image under $g(\cdot)$ is an open ball in \mathcal{R}^m centered at r with radius $\rho > 0$, denoted by $B(r, \rho)$. Furthermore, assume that the function $g : \Omega \rightarrow B(r, \rho)$ is bijective, and both it and its inverse have bounded first derivatives (Jacobians) on Ω and $B(r, \rho)$, respectively. The existence of sets satisfying these assumptions is ensured by the inverse-function theorem.

Consider an application of the controller, defined by (6), on Ω . Define the Lyapunov function

$$V(u(t)) := \frac{1}{2} \|r(t) - g(u(t))\|^2, \quad (7)$$

with $r(t) \equiv r$. It follows from (6) and some algebra that $\dot{V}(t) = -\|r - g(u(t))\|^2 = -2V(t)$ thereby guaranteeing local convergence in the sense of Eq. (5). However, if r is not in the range of the function $g(\cdot)$, the computed control-trajectory $\{u(t) : t \in [0, \infty)\}$ may be unbounded. For example, consider the one-dimensional system where $g(u) = \arctan(u)$, rendering (6) with $r(t) \equiv r$ as

$$\dot{u}(t) = (u(t)^2 + 1) (r - \arctan(u(t))).$$

If $r \in (-\frac{\pi}{2}, \frac{\pi}{2})$, then Eq. (7) guarantees that $g(u(t)) \rightarrow r$ as $t \rightarrow \infty$, with a global domain of attraction. If $r = \frac{\pi}{2}$, the limit $g(u(t)) \rightarrow r$ still holds but $u(t) \rightarrow \infty$; in a sense we have tracking but not stability. Finally, if $|r| > \frac{\pi}{2}$, the above differential equation has a finite escape time where $u(t) \rightarrow \infty$. Thus, tracking and stability, in the sense of Eq. (5) and the boundedness of the control trajectory $\{u(t) : t \in [0, \infty)\}$, depend on a proper choice of the target reference. We point out that for systems whose plant is a continuously-differentiable memoryless nonlinearity as in (3), with a controller defined by (6) for a constant reference, global tracking and stability are assured as long as the function $V(\cdot)$, defined by Eq. (7), is proper in the sense that it has bounded level sets, and the Jacobian $\frac{\partial g}{\partial u}(u)$ is nonsingular for all $u \in \mathcal{R}^m$. These are strong assumptions, made more difficult to prove when the plant is a dynamical system. Therefore we later will focus a part of the discussion on a suitable notion of local stability and tracking. However, we will prove a global stability for a class of linear systems.

Next, let us return the discussion to the case where the target reference is a function of time, $r(t)$, and suppose that it is bounded, continuous, and piecewise-continuously differentiable. The system is defined by Eq. (3), and the control is defined by Eq. (6). Even if the control trajectory $\{u(t) : t \in [0, \infty)\}$ is well defined, bounded, continuous and piecewise-continuously differentiable, and the inverse-Jacobian $\left(\frac{\partial g}{\partial u}(u(t))\right)^{-1}$ along it is bounded, the convergence defined by Eq. (5) is not guaranteed. Instead, we have

$$\limsup_{t \rightarrow \infty} \|r(t) - y(t)\| \leq \eta, \quad (8)$$

where $\eta := \limsup_{t \rightarrow \infty} \|\dot{r}(t)\|$ (see [16]). To tighten the upper bound in (8), we can speed up the action of the controller. One way to do it is to multiply the Right-Hand Side (RHS) of Eq. (6) by a constant $\alpha > 1$, which results in the following equation,

$$\dot{u}(t) = \alpha \left(\frac{\partial g}{\partial u}(u(t))\right)^{-1} (r(t) - g(u(t))). \quad (9)$$

This gives the following bound,

$$\limsup_{t \rightarrow \infty} \|r(t) - y(t)\| \leq \frac{\eta}{\alpha}, \quad (10)$$

under suitable stability assumptions as defined in the sequel.

This paper considers the plant subsystem to be a dynamical system defined by an ordinary differential equation. Accordingly, let $x(t) \in \mathcal{R}^n$ denote its state variable modelled by the equation

$$\dot{x}(t) = f(x(t), u(t)), \quad (11)$$

where $u(t) \in \mathcal{R}^m$ is the control input, $f : \mathcal{R}^n \times \mathcal{R}^m \rightarrow \mathcal{R}^n$ is a suitable function, $t \in [0, \infty)$, and a given $x(0) := x_0 \in \mathcal{R}^n$ is the initial state. The output function is

$$y(t) = h(x(t)), \quad (12)$$

where $y(t) \in \mathcal{R}^m$, for a function $h : \mathcal{R}^n \rightarrow \mathcal{R}^m$. We make the following assumptions on the functions f and h :

Assumption 1. 1). The function $f : \mathcal{R}^n \times \mathcal{R}^m \rightarrow \mathcal{R}^n$ is continuously differentiable, and for every compact set $\Gamma \subset \mathcal{R}^m$ there exists $K > 0$ such that, for every $(x, u) \in \mathcal{R}^n \times \Gamma$,

$$\|f(x, u)\| \leq K(\|x\| + 1). \quad (13)$$

2). The function $h : \mathcal{R}^n \rightarrow \mathcal{R}^m$ is continuously differentiable.

Assumption 1 guarantees the existence of a unique continuous, piecewise-differentiable solution for Eq. (11) on the time-horizon $\{t : t \geq 0\}$, as long as the input $u(t)$ is piecewise continuous and bounded.

Extensions of the controller defined in (9) from the case of memoryless plants to that of dynamic plants raises a few challenges. To start with, the input-to-output relation cannot be expressed in an algebraic-functional form like in Eq. (3), because $x(t)$, hence $y(t)$ are not functions of $u(t)$ but of $\{u(\tau) : \tau < t\}$. Therefore the controller cannot be defined by an equation like (9). We resolve this issue with the use of an output predictor $\hat{y}(t+T)$, assumed to have the functional form

$$\hat{y}(t+T) := g(x(t), u(t)), \quad (14)$$

for a suitable function $g : \mathcal{R}^n \times \mathcal{R}^m \rightarrow \mathcal{R}^m$ and a fixed prediction horizon $T > 0$. The predictor that we use will be presented below, and evidently it has the format of Eq. (14).

Assumption 2. The function $g(\cdot, \cdot)$ is continuously differentiable in (x, u) , and its partial Jacobian, $\frac{\partial g}{\partial u}(x, u)$ is locally Lipschitz continuous in $(x, u) \in \mathcal{R}^{n+m}$.

Recall that $r(t+T)$ is the target of tracking by $\hat{y}(t+T) = g(x(t), u(t))$. To this end, we extend the Newton-Raphson flow from Eq. (9) to the following equation,

$$\dot{u}(t) = \alpha \left(\frac{\partial g}{\partial u}(x(t), u(t)) \right)^{-1} (r(t+T) - g(x(t), u(t))), \quad (15)$$

which we use to define the tracking controller. Putting together the state equation (11) with the control equation (15), we obtain the joint equation

$$\begin{cases} \dot{x}(t) = f(x(t), u(t)), \\ \dot{u}(t) = \alpha \left(\frac{\partial g}{\partial u}(x(t), u(t)) \right)^{-1} (r(t+T) - g(x(t), u(t))), \end{cases} \quad (16)$$

which has been viewed in [18] as the state equation of an $n + m$ -dimensional dynamical system with the augmented state $z(t) := (x(t)^\top, u(t)^\top)^\top \in \mathcal{R}^{n+m}$ and the input $r(t+T) \in \mathcal{R}^m$. We remark that, given an initial condition $z_0 := (x_0^\top, u_0^\top)^\top$ for (16) such that $\frac{\partial g}{\partial u}(x_0, u_0)$ is nonsingular, Assumption 1 and Assumption 2 imply the existence of a unique continuous, piecewise-differentiable solution to Eq. (16) on some time-interval $[0, t_1)$. Furthermore, denoting by $[0, \hat{t}_1)$ the maximal interval of such a solution, $\hat{t}_1 = \infty$ unless the trajectory $\{(x(t)^\top, u(t)^\top)^\top : t \in [0, \hat{t}_1)\}$ is unbounded, or its closure contains a point where $\frac{\partial g}{\partial u}(x(t), u(t))$ is singular.

The controller defined by (15) was presented in [15] with the particular predictor defined as follows: At time t , given $x(t)$ and $u(t)$, let $\{\xi(\tau) : \tau \in [t, t+T]\}$ be defined by the differential equation

$$\dot{\xi}(\tau) = f(\xi(\tau), u(t)) \quad (17)$$

with the boundary condition $\xi(t) = x(t)$; then define

$$\hat{y}(t+T) := g(x(t), u(t)) = h(\xi(t+T)). \quad (18)$$

Observe that Eq. (17) is essentially the state equation (11) except that it is defined only on the interval $\tau \in [t, t+T]$ with the constant input $u(\tau) \equiv u(t)$ and the initial condition $\xi(t) = x(t)$. We typically solved Eq. (17) by the forward Euler method.

Ref. [15] examined the Bounded-Input-Bounded-State (BIBS) stability of the system defined by (16), with the predictor defined by (17)-(18), on a number of examples of second-order systems. It was shown that, for a fixed $\alpha > 0$, the systems are BIBS stable for a large T but unstable for a small T . Now a small T may be desirable since it results in a smaller prediction error than larger T . To circumvent this conundrum, it was demonstrated for the above examples that for every fixed $T > 0$, the closed-loop system can be stabilized by increasing α . Moreover, simulation results suggest that the following extension of Eq. (10),

$$\limsup_{t \rightarrow \infty} \|r(t) - \hat{y}(t)\| < \frac{\eta}{\alpha}, \quad (19)$$

is satisfied under general assumptions. Thus, a controller's speedup by choosing a large α in Eq. (15) may serve the dual purpose of stabilizing the closed-loop system if need be, and reducing the asymptotic tracking error. We point out that stabilizability by increasing α , though observed in the aforementioned examples, generally is not guaranteed. The derivation of sufficient conditions for it in general is quite challenging since the function $g(x, u)$ lacks a closed form, but some results will be presented for linear systems in Section 4.

Finally, a word must be said about the differences between the proposed technique and Model-Predictive Control. MPC uses optimal control over rolling horizons to compute a future target trajectory as well as the control input to track it. Our technique is not concerned with the computation of the reference trajectory but only with its tracking, for which it uses a Newton-Raphson flow, not optimal control. If the reference trajectory has to be computed in real time then various numerical techniques can be used including interpolation as in Section 5, below, or learning methods based on neural nets as in ([19, 4]).

3 | CONVERGENCE ANALYSIS

Consider a system defined by Eqs. (11) and (12) under Assumption 1, and suppose that the predictor, defined by (14), satisfies Assumption 2. This section derives theoretical results concerning asymptotic convergence of the tracking-control algorithm defined by Eq. (15) and variations thereof. We generalize Eq. (15) to the following form,

$$\dot{u}(t) = \left(\frac{\partial g}{\partial u}(x(t), u(t)) \right)^{-1} \left(\alpha(r(t+T) - g(x(t), u(t))) + E(x(t), u(t), t) \right), \quad (20)$$

where the function $E : \mathcal{R}^n \times \mathcal{R}^m \times \mathcal{R}^+ \rightarrow \mathcal{R}^m$ is locally Lipschitz continuous in $(x^\top, u^\top)^\top \in \mathcal{R}^n \times \mathcal{R}^m$ and piecewise continuous in $t \in \mathcal{R}^+$. Note that the difference between (15) and (20) is in the inclusion of the term $E(x(t), u(t), t)$ in the RHS of (20), and this term is not multiplied by α . Various controllers will be defined according to specific forms of $E(x(t), u(t), t)$, and their related asymptotic tracking errors will be analyzed. We first propose a particular feed-forward term that gives zero asymptotic tracking error. Next, we carry out an error analysis with the objective of identifying the kinds of additive errors whose effects can be reduced by increasing α vs. those which might not be directly affected by α . Lastly, we explore general relationships between stability and asymptotic tracking. We point out that most of the proofs in this section, though perhaps technically involved, are based on fairly straightforward arguments from the theory of Lyapunov's direct method; this is due to the particular dynamics of the Newton-Raphson flow for solving algebraic equations.

Central to the analysis is a suitable notion of a system's stability, which must include the requirement that state trajectories preclude points $(x^\top, u^\top)^\top \in \mathcal{R}^{n+m}$ where the partial-Jacobian matrix $\frac{\partial g}{\partial u}(x(t), u(t))$ is singular. Another source of a system's instability is due to the dynamics of Eq. (16) in the variable $(x^\top, u^\top)^\top \in \mathcal{R}^{n+m}$. Regarding the latter, as mentioned in the last section, increasing the controller's rate α may stabilize the closed-loop system and reduce the tracking error. Therefore, we will focus the analysis on tracking at large α and define the stability concept, called α -stability, to aid in this regard. We will derive a verifiable sufficient condition for α -stability of linear systems in Section 4. However, for general nonlinear systems we doubt that a single practically-verifiable sufficient condition can be derived, and instead, α -stability may have to be proved for classes of systems having special properties. Even then the derivation of proofs may be quite challenging, especially if the prediction function $g(x, u)$ does not have a closed form. Therefore the concept of α -stability will be defined in a way that can represent local stability, which may be easier to analyze, as well as global stability, as for linear systems. *In this section (and paper) we do not attempt to prove α -stability for nonlinear systems; we define and discuss the concept, use it to derive results concerning tracking, and demonstrate it (and the related tracking) via simulation and in the lab on various examples in Sections 5 and 6. Proofs for particular systems will be presented in subsequent publications.*

To introduce the notion of stability we first establish some notation. Consider the closed-loop system defined by Eqs. (11), (12), and (20). As indicated following Eq. (16), it can be viewed as a dynamical system with the augmented-state variable $z(t) := (x(t)^\top, u(t)^\top)^\top \in \mathcal{R}^{n+m}$, input $r(t) \in \mathcal{R}^m$, and output $y(t) \in \mathcal{R}^m$. Denote by C the space of bounded, continuous functions $r : [0, \infty) \rightarrow \mathcal{R}^m$ having a piecewise-continuous, bounded derivative $\dot{r}(t)$. We henceforth assume that the target-reference function $\{r(t) : t \in [0, \infty)\}$ is contained in C . Denote by $L^\infty(\mathcal{R}^m)$ the space of essentially-bounded functions $p : [0, \infty) \rightarrow \mathcal{R}^m$, and by $\|p\|_\infty$, the L^∞ norm of $p \in L^\infty(\mathcal{R}^m)$. Fix $\alpha > 0$. We say that, for a given initial condition $z_0 \in \mathcal{R}^{n+m}$, the state trajectory $\{z(t) : t \in [0, \infty)\}$ is *well-defined* if it comprises the unique continuous, piecewise-continuously differentiable solution of Eqs. (11) and (20) (jointly) over $t \in [0, \infty)$, with the initial condition $z(0) = z_0$. A well-defined state trajectory is said to be *nonsingular* if for every $z(t) := (x(t)^\top, u(t)^\top)^\top$ contained in it, the partial Jacobian $\frac{\partial g}{\partial u}(x(t), u(t))$ is nonsingular. Finally, we use the shorthand notation $\{z(t)\}$ for a state trajectory $\{z(t) : t \in [0, \infty)\}$ that is well defined, and similarly for the trajectories $\{x(t)\}$, $\{u(t)\}$, $\{y(t)\}$ and $\{r(t)\}$.

α -stability is defined with respect to given open set $\Omega \subset L^\infty(\mathcal{R}^m)$ and closed set $\Gamma \subset \mathcal{R}^{n+m}$, as follows.

Definition 1. Given an open set $\Omega \subset L^\infty(\mathcal{R}^m)$ and a closed set $\Gamma \subset \mathcal{R}^{n+m}$, the system defined by (11), (20) and (12) is α -stable with respect to Ω and Γ if there exist $\bar{\alpha} > 0$, and two continuous, monotone-nondecreasing functions $\gamma : \mathcal{R}^+ \rightarrow \mathcal{R}^+$ and $\beta : \mathcal{R}^+ \rightarrow \mathcal{R}^+$, such that for every $\alpha > \bar{\alpha}$, and for every reference input $\{r(t)\} \in \Omega \cap C$ and an initial condition $z_0 := z(0) \in \Gamma$, the trajectory $\{z(t)\}$ is well defined and nonsingular, and the following equation is satisfied,

$$\|z\|_\infty \leq \gamma(\|r\|_\infty) + \beta(\|z_0\|). \quad (21)$$

Note that the state trajectory $\{z(t)\}$ in (21) depends on $\{r(t)\}$ and z_0 as well as $\alpha > 0$, but the latter dependence is suppressed in the used notation for the sake of simplicity of presentation. Moreover, the right-hand side of (21) is independent on α as long as the target-reference process $\{r(t)\}$ is exogenous, but may be α -dependent if $\{r(t)\}$ is endogenous; more on that will be said later.

We remark that if $\Omega = L^\infty(\mathcal{R}^m)$ and $\Gamma = \mathcal{R}^m$ then α -stability can be thought of as a global concept. On the other hand, if Ω is a sleeve around a target reference $\{\hat{r}(t)\}$, namely $\Omega = \{r \in L^\infty : \|r - \hat{r}\|_\infty < \rho\}$ for a given $\rho > 0$, and Γ is a closed ball centered at a point $\hat{z}_0 \in \mathcal{R}^{n+m}$, then α -stability has a local meaning. A practical scenario may arise when it is known that a given target trajectory $\{\hat{r}(t)\} \in C$ gives a well-defined, nonsingular, bounded trajectory $\{\hat{z}(t)\}$, and it is desirable to prove that these properties also are satisfied in a sleeve around $\{\hat{r}(t)\}$ and a compact set of possible initial conditions including $\hat{z}(0)$.

We start the analysis in this section by considering a modification of the controller defined by (15) which gives zero asymptotic tracking error at fixed values of α . We then investigate the effects of additive errors in the loop on the asymptotic tracking. Lastly, we prove asymptotic tracking from α -stability in a general setting. The α -stability assumption is not required for the first two parts of the analysis, where we use a weaker assumption. It is, however, needed in the last part where the setting for the analysis is more general.

3.1 | Enhanced Controller

Consider the closed-loop system defined by Eqs. (11), (12) and the following controller equation,

$$\dot{u}(t) = \left(\frac{\partial g}{\partial u}(x(t), u(t)) \right)^{-1} \left(\alpha(r(t+T) - \hat{y}(t+T)) + \dot{r}(t+T) - \frac{\partial g}{\partial x}(x(t), u(t))f(x(t), u(t)) \right), \quad (22)$$

where it is assumed that $\{r(t)\} \in C$. Note that (22) is a special case of (20) with

$$E(x(t), u(t), t) = \dot{r}(t+T) - \frac{\partial g}{\partial x}(x(t), u(t))f(x(t), u(t)). \quad (23)$$

Fix a predictor's horizon $T > 0$, a controller's rate $\alpha > 0$, and an initial condition $z_0 = z(0) \in \mathcal{R}^{n+m}$.

Define the function $V(x(t), u(t))$ by

$$V(x(t), u(t)) := \frac{1}{2} \|r(t+T) - \hat{y}(t+T)\|^2. \quad (24)$$

Proposition 1. Suppose that Assumption 1 and Assumption 2 are satisfied. If the trajectory $\{z(t)\}$ is well-defined, nonsingular and bounded, then $V(x(t), u(t))$ satisfies the following equation,

$$\dot{V}(x(t), u(t)) = -2\alpha V(x(t), u(t)), \quad (25)$$

and consequently,

$$\lim_{t \rightarrow \infty} (r(t) - \hat{y}(t)) = 0. \quad (26)$$

Proof. Taking derivatives with respect to t in (24), and considering the fact that $\hat{y}(t+T) = g(x(t), u(t))$,

$$\dot{V}(x(t), u(t)) = \left\langle r(t+T) - \hat{y}(t+T), \dot{r}(t+T) - \frac{d}{dt}g(x(t), u(t)) \right\rangle. \quad (27)$$

Next, by Eqs. (11) and (22),

$$\begin{aligned} \frac{d}{dt}g(x(t), u(t)) &= \frac{\partial g}{\partial x}(x(t), u(t))f(x(t), u(t)) \\ &+ \frac{\partial g}{\partial u}(x(t), u(t)) \left(\frac{\partial g}{\partial u}(x(t), u(t)) \right)^{-1} \left(\alpha(r(t+T) - g(x(t), u(t))) + \dot{r}(t+T) - \frac{\partial g}{\partial x}(x(t), u(t))f(x(t), u(t)) \right). \end{aligned} \quad (28)$$

Lastly, simplifying and applying Eq. (28) to (27), Eq. (25) is obtained, whence Eq. (26) follows. \square

We remark that Proposition 3.2 holds true and its proof is valid regardless of whether the process $\{r(t+T)\}$ is exogenous or functionally dependent on $\{z(t)\}$ via feedback. In the latter case this dependence must be reflected in the computation of $\dot{r}(t+T)$ required by Eq. (22).

3.2 | Error Analysis

This subsection considers three types of potential additive errors in the loop, added to various terms in the RHS of Eq. (22), and evaluates their effects on the tracking performance.

3.2.1 | Prediction error.

Fix $\alpha > 0$. Consider the prediction error defined as $\mathcal{E}_1(t) := \hat{y}(t+T) - y(t+T)$, and define the asymptotic prediction error by

$$\eta_1 := \limsup_{t \rightarrow \infty} \|\mathcal{E}_1(t)\|. \quad (29)$$

η_1 may depend on α , but we suppress this dependence in the notation used. Under the assumptions made for Proposition 1, Eq. (26) implies that

$$\limsup_{t \rightarrow \infty} \|r(t) - y(t)\| = \eta_1. \quad (30)$$

Defining the asymptotic tracking error by the Left-hand Side (LHS) of (30), we see that the asymptotic prediction error is translated to the asymptotic tracking error regardless of the value of $\alpha > 0$.

3.2.2 | Error in $\dot{r}(t + T) - \frac{\partial g}{\partial x}(x(t), u(t))f(x(t), u(t))$.

Fix $\alpha > 0$. Let $\mathcal{E}_2(t)$ denote an error added to the term $\dot{r}(t + T) - \frac{\partial g}{\partial x}(x(t), u(t))f(x(t), u(t))$ in the RHS of Eq. (22). Due to this error, the controller equation is modified from (22) to the following equation,

$$\dot{u}(t) = \left(\frac{\partial g}{\partial u}(x(t), u(t)) \right)^{-1} \left(\alpha(r(t + T) - \hat{y}(t + T)) + \dot{r}(t + T) - \frac{\partial g}{\partial x}(x(t), u(t))f(x(t), u(t)) + \mathcal{E}_2(t) \right). \quad (31)$$

Define

$$\eta_2 := \limsup_{t \rightarrow \infty} \|\mathcal{E}_2(t)\|. \quad (32)$$

$\mathcal{E}_2(t)$ may depend on α , but this dependence is suppressed in the notation used.

Proposition 2. Suppose that Assumption 1 and Assumption 2 are satisfied. Consider the closed-loop system defined by Eqs. (11), (12), and (31) with a fixed $\alpha > 0$, with a given initial condition $z_0 \in \mathcal{R}^{n+m}$. Suppose that the resulting trajectory $\{z(t)\}$ is well defined, nonsingular and bounded over all $t \in [0, \infty)$. Then,

$$\limsup_{t \rightarrow \infty} \|r(t) - \hat{y}(t)\| \leq \frac{\eta_2}{\alpha}. \quad (33)$$

Proof. If $\eta_2 = \infty$ then (33) is obvious. Consider the case where $\eta_2 < \infty$. Define the function $V(x(t), u(t))$ by Eq. (24). Taking derivatives with respect to t , and recalling that $\hat{y}(t + T) = g(x(t), u(t))$, we have that

$$\dot{V}(x(t), u(t)) = \left\langle r(t + T) - \hat{y}(t + T), \dot{r}(t + T) - \frac{d}{dt}g(x(t), u(t)) \right\rangle. \quad (34)$$

By Eqs. (11) and (31), after some algebra we obtain that

$$\begin{aligned} \frac{d}{dt}g(x(t), u(t)) &= \frac{\partial g}{\partial x}(x(t), u(t))f(x(t), u(t)) \\ &+ \alpha(r(t + T) - \hat{y}(t + T)) + \dot{r}(t + T) - \frac{\partial g}{\partial x}(x(t), u(t))f(x(t), u(t)) + \mathcal{E}_2(t). \end{aligned} \quad (35)$$

Using Eq. (35) in Eq. (34) we obtain,

$$\dot{V}(x(t), u(t)) = \left\langle r(t + T) - \hat{y}(t + T), -\alpha(r(t + T) - \hat{y}(t + T)) - \mathcal{E}_2(t) \right\rangle. \quad (36)$$

Consequently, for given $\epsilon > 0$ and $t \geq 0$, if $\alpha\|r(t + T) - \hat{y}(t + T)\| > \|\mathcal{E}_2(t)\| + \epsilon$, then (36) and the Cauchy-Schwarz inequality imply that $\dot{V}(x(t), u(t)) \leq -\epsilon\|r(t + T) - \hat{y}(t + T)\|$. By (24), $\|r(t + T) - \hat{y}(t + T)\| = (2V(x(t), u(t)))^{1/2}$. Therefore, some algebra and the latest inequality mean that if $\alpha(2V(x(t), u(t)))^{1/2} > \|\mathcal{E}_2(t)\| + \epsilon$, then

$$\frac{d}{dt} \left((2V(x(t), u(t)))^{1/2} \right) \leq -\epsilon. \quad (37)$$

This implies that $\alpha \limsup_{t \rightarrow \infty} \|r(t) - \hat{y}(t)\| \leq \|\mathcal{E}_2\| + \epsilon$, and since $\epsilon > 0$ was arbitrary, Eq. (33) follows. \square

We point out that Proposition 2 holds true and its proof is valid regardless of whether either process $\{r(t + T)\}$ or $\{\mathcal{E}_2(t)\}$ is exogenous or functionally dependent on $\{z(t)\}$ via feedback. Of course, in the latter case it may be difficult to prove the assumptions underscoring the proposition.

Recall the definition of the asymptotic prediction error, η_1 , by Eq. (29).

Corollary 1. Under the assumptions of Proposition 2,

$$\limsup_{t \rightarrow \infty} \|r(t) - y(t)\| \leq \eta_1 + \frac{\eta_2}{\alpha}. \quad (38)$$

Proof. It follows directly from Proposition 2 and the definition of η_1 . \square

The enhanced controller, defined by Eq. (22), seems to have better convergence than the more-basic controller defined by Eq. (15). However, the latter controller still has a place since it is simpler, and also can be more practical in situations where $r(t + T)$

is computed in real time (at time t) but $\dot{r}(t+T)$ cannot be computed at that time. An intermediate control algorithm between (15) and (22), defined by Eq. (39), is also possible.

$$\dot{u}(t) = \left(\frac{\partial g}{\partial u}(x(t), u(t)) \right)^{-1} \left(\alpha(r(t+T) - \hat{y}(t+T)) - \frac{\partial g}{\partial x}(x(t), u(t))f(x(t), u(t)) \right). \quad (39)$$

For the purpose of analysis, the controllers based on Eqs. (15), (22) and (39) can be viewed as special cases of the controller defined by (31) by setting $\mathcal{E}_2(t) := -\dot{r}(t+T) + \frac{\partial g}{\partial x}(x(t), u(t))$, $\mathcal{E}_2(t) := 0$, and $\mathcal{E}_2(t) = -\dot{r}(t+T)$, respectively.

3.2.3 | Error in $\left(\frac{\partial g}{\partial u}(x(t), u(t)) \right)^{-1}$.

Convergence of the standard Newton-Raphson method for solving nonlinear equations is known to be robust to errors in the computation of the inverse-Jacobian (see, e.g., [20], Section 1.4.3). A similar robustness holds for convergence of the controller defined by Eq. (31) with respect to errors in the term $\left(\frac{\partial g}{\partial u}(x(t), u(t)) \right)^{-1}$, and Eq. (33) still holds if such errors are small enough. Therefore we henceforth implicitly assume that the inverse-Jacobian in Eq. (31) is exact.

3.3 | Stability as a Sufficient Condition for Tracking

This subsection explores a relationship between the α -stability of a system and its asymptotic tracking as $\alpha \rightarrow \infty$. The analysis is carried out under the assumption that the target-reference signal $\{r(t)\}$ is exogenous and hence independent of α , but comments will be offered on its possible extensions to the case where $\{r(t)\}$ depends on $\{z(\tau)\}$ via feedback.

Proposition 3. Consider the closed-loop system defined by Eqs. (11)-(12) with the controller defined by either equation (15), (22), or (39). Suppose that Assumption 1 and Assumption 2 are satisfied. Given an open set $\Omega \subset L^\infty(\mathcal{R}^m)$ and a closed set $\Gamma \subset \mathcal{R}^{n+m}$, suppose that the system is α -stable with respect to Ω and Γ . Then for every exogenous reference input $\{r(t)\} \in \Omega \cap C$, and for every $z_0 \in \Gamma$,

$$\lim_{\alpha \rightarrow \infty} \limsup_{t \rightarrow \infty} \|r(t) - \hat{y}(t)\| = 0. \quad (40)$$

Proof. Consider first the case where the controller is defined by Eq. (22). By Definition 1, there exists $\bar{\alpha} > 0$ such that for every $\alpha > \bar{\alpha}$, for every $\{r(t)\} \in \Omega \cap C$ and for every $z_0 \in \Gamma$, the closed-loop state trajectory $\{z(t)\}$ is well defined, nonsingular and bounded. By Proposition 1, Eq. (26) is in force, hence (40) is satisfied as well.

Next, consider the controller defined by Eq. (15). It is equivalent to Eq. (31) with $\mathcal{E}_2(t) = -\dot{r}(t+T) + \frac{\partial g}{\partial x}(x(t), u(t))f(x(t), u(t))$. Suppose that the closed-loop system is α -stable with respect to an open set $\Omega \subset L^\infty(\mathcal{R}^m)$ and a closed set $\Gamma \subset \mathcal{R}^{n+m}$. By Definition 1, there exist $\bar{\alpha} > 0$, and two continuous, monotone-nondecreasing functions $\gamma : \mathcal{R}^+ \rightarrow \mathcal{R}^+$ and $\beta : \mathcal{R}^+ \rightarrow \mathcal{R}^+$, such that, for every $\{r(t)\} \in \Omega \cap C$, $z_0 \in \Gamma$, and $\alpha > \bar{\alpha}$, Eq. (21) is satisfied. Now consider an exogenous process $\{r(t)\} \in \Omega \cap C$ and $z_0 \in \Gamma$. Since $\{r(t)\}$ is exogenous it is independent of α , hence the RHS of (21) is also independent of α ; and by (32), η_2 is independent of α as well. Therefore, and by Proposition 2, Eq. (40) follows.

Finally, the case where the controller is defined by Eq. (39) follows the same argument, in a simpler form since it corresponds to (31) with $\mathcal{E}_2(t) = -\dot{r}(t+T)$. \square

We remark that Proposition 3 perhaps may be extendable from the case where the reference target $\{r(t)\}$ is exogenous to the case where it is controlled and hence dependent on α . This requires that η_2 , defined by (32), though dependent on α , be upper-bounded by a constant that is independent of α . The validity of this property and its proof are expected to depend on specific properties of a system under study.

We conclude this section by summarizing the scope of the results derived therein. Broadly, they analyze the asymptotic tracking errors for various controllers based on the Newton-Raphson flow, and assert that tracking can be a consequence of α -stability. The proofs are based on variants of Lyapunov's direct method. The next section provides a verifiable sufficient condition for α -stability, hence tracking convergence for a class of linear systems.

4 | LINEAR SYSTEMS

Consider the special case where the plant is a linear, time-invariant system of the form

$$\dot{x}(t) = Ax(t) + Bu(t), \quad y(t) = Cx(t), \quad (41)$$

where $A \in \mathcal{R}^{n \times n}$, $B \in \mathcal{R}^{n \times m}$, and $C \in \mathcal{R}^{m \times n}$ are given matrices. Suppose that $\hat{y}(t+T)$ is defined by Eqs. (17)-(18), and that the controller is defined by either Eq. (15), (22) or (39). The respective analyses of these controllers are almost identical, hence we perform a detailed analysis only for the case of (15) and point out in context the required modifications for the two other cases. Furthermore, to simplify the exposition we assume that A is nonsingular which makes possible the term $A^{-1}(e^{AT} - I)$ in Eq. (42), below; we will comment in the sequel on the case where A is singular.

Fix $T > 0$. By Eqs. (17)-(18), we have that

$$g(x(t), u(t)) = Ce^{AT}x(t) + CA^{-1}(e^{AT} - I)Bu(t), \quad (42)$$

where I denotes the identity matrix. Therefore,

$$\frac{\partial g}{\partial x}(x(t), u(t)) = Ce^{AT}, \quad (43)$$

and

$$\frac{\partial g}{\partial u}(x(t), u(t)) = CA^{-1}(e^{AT} - I)B. \quad (44)$$

Since $\frac{\partial g}{\partial u}(x(t), u(t))$ is a constant (independent of t) matrix, we conclude that the matrix $CA^{-1}(e^{AT} - I)B$ is nonsingular if and only if every trajectory of the system is nonsingular regardless of the target reference $\{r(t)\}$ or the initial condition z_0 . Therefore, we will assume that the matrix $CA^{-1}(e^{AT} - I)B$ is nonsingular. Furthermore, Assumption 1 and Assumption 2 follow from Eqs. (41) and (42), respectively. Consequently, by Proposition 3, tracking in the sense of (40) would follow from the α -stability of the system, and we will derive a sufficient condition for α -stability with respect to $\Omega := L^\infty(\mathcal{R}^m)$ and $\Gamma = \mathcal{R}^{n+m}$. We formalize the above assumptions which are held to be implicit throughout the following analysis.

Assumption 3. The matrices A and $CA^{-1}(e^{AT} - I)B$ are nonsingular.

With the controller defined by (15), the closed-loop system has the form of Eq. (16). By Eqs. (15) and (42)-(44) the controller has the following form,

$$\dot{u}(t) = \alpha \left(CA^{-1}(e^{AT} - I)B \right)^{-1} r(t+T) - \alpha \left(CA^{-1}(e^{AT} - I)B \right)^{-1} Ce^{AT}x(t) - \alpha u(t). \quad (45)$$

Therefore Eq. (16) assumes the form

$$\begin{pmatrix} \dot{x}(t) \\ \dot{u}(t) \end{pmatrix} = \Phi_\alpha \begin{pmatrix} x(t) \\ u(t) \end{pmatrix} + \Psi_\alpha r(t+T), \quad (46)$$

where Φ_α is an $(n+m) \times (n+m)$ matrix having the following block structure,

$$\Phi_\alpha = \begin{pmatrix} A & B \\ -\alpha \left(CA^{-1}(e^{AT} - I)B \right)^{-1} Ce^{AT} & -\alpha I \end{pmatrix}, \quad (47)$$

and Ψ_α is an $(n+m) \times n$ matrix of the form

$$\Psi_\alpha = \begin{pmatrix} 0 \\ \alpha \left(CA^{-1}(e^{AT} - I)B \right)^{-1} \end{pmatrix}, \quad (48)$$

where the block of zeros is $n \times n$.

We remark that in the event that the matrix A is singular, Eq. (44) is no-longer valid. In this case, as long as the matrix $\frac{\partial g}{\partial u}(x, u) \in \mathcal{R}^{m \times m}$ is nonsingular, it can replace the term $CA^{-1}(e^{AT} - I)B$ in both (47) and (48) to ensure that the rest of the analysis in this section is applicable.

Returning to Eq. (47), observe that α multiplies the last m rows of Φ_α but none of its first n rows, and hence we can write Φ_α in the following way,

$$\Phi_\alpha = \begin{pmatrix} \phi_{1,1} & \phi_{1,2} & \cdots & \phi_{1,n+m} \\ \phi_{2,1} & \phi_{2,2} & \cdots & \phi_{2,n+m} \\ \cdot & \cdot & \cdots & \cdot \\ \cdot & \cdot & \cdots & \cdot \\ \phi_{n,1} & \phi_{n,2} & \cdots & \phi_{n,n+m} \\ \alpha\phi_{n+1,1} & \alpha\phi_{n+1,2} & \cdots & \alpha\phi_{n+1,n+m} \\ \cdot & \cdot & \cdots & \cdot \\ \cdot & \cdot & \cdots & \cdot \\ \alpha\phi_{n+m,1} & \alpha\phi_{n+m,2} & \cdots & \alpha\phi_{n+m,n+m} \end{pmatrix} \quad (49)$$

for some scalars $\phi_{j,i}$, $j = 1, \dots, n+m$; $i = 1, \dots, n+m$. The determinant of $sI - \Phi_\alpha$ is a two-dimensional polynomial in α and s , which we denote by $P(s; \alpha)$. The standard formula for computing determinants reveals the following result, whose proof can be found in ([18], Lemma 4.3).

Lemma 1. For every $i = 1, \dots, m$ there exists a polynomial $P_i(s)$ of degree no more than $n+i$, such that,

$$P(s; \alpha) = \sum_{i=0}^m \alpha^i P_{m-i}(s). \quad (50)$$

Remark 1. For the cases where the controller is defined by either (22) or (39), the only resulting change to Φ_α is that the entries of its last m rows are first-order polynomials in α with possibly-nonzero free coefficients (currently they are first-order polynomials whose free coefficients are 0). That would not affect the validity of Lemma 1 or the rest of the analysis in this section.

Since by assumption $\deg(P_i) \leq n+i$, we can write $P_i(s)$ as

$$P_i(s) = \sum_{j=0}^{n+i} a_{i,j} s^j \quad (51)$$

for some coefficients $a_{i,j}$, $j = 0, \dots, n+i$. We assume, for simplicity of presentation, that $a_{i,n+i} \neq 0$ to ensure that $\deg(P_i) = n+i$. Then

$$P(s; \alpha) = \sum_{i=0}^m \alpha^i \sum_{j=0}^{n+m-i} a_{m-i,j} s^j. \quad (52)$$

Since $P(s; \alpha)$ is the characteristic polynomial of a matrix, the coefficient of its highest order in s is 1. This coefficient, corresponding to $i = 0$ and $j = n+m$ in (52), is $a_{m,n+m}$; hence $a_{m,n+m} = 1$.

Define $\Omega = L^\infty(\mathcal{R}^m)$, and let $\Gamma := \mathcal{R}^{n+m}$. The sufficient condition for α -stability with respect to Ω and Γ , derived below, amounts to two polynomials, expressed in terms of the system's parameters, having all of their roots in the Left-Half Plane (LHP). One polynomial has degree n , the other has degree m , and both are independent of α hence the sufficient condition is verifiable.

The first polynomial is $P_0(s)$, which by (50) is the polynomial-coefficient of α^m , the leading term in $P(s; \alpha)$ in terms of the power of α . Note (Eq. (51)) that $\deg(P_0) = n$.

The second polynomial, denoted by $Q(s)$, is defined as follows. For every $i = 0, \dots, m$, consider the polynomial $P_i(s)$, defined in Eq. (51), whose degree is $n+i$. Define the polynomial $\tilde{P}_i(s)$ as the monomial consisting of the highest-order term of $P_i(s)$, namely,

$$\tilde{P}_i(s) = a_{i,n+i} s^{n+i}. \quad (53)$$

Next, in analogy to (50), define the family of polynomials parameterized by $\alpha > 0$, $\{\tilde{P}(s; \alpha)\}$, by

$$\tilde{P}(s; \alpha) = \sum_{i=0}^m \alpha^i \tilde{P}_{m-i}(s). \quad (54)$$

By (53),

$$\tilde{P}(s; \alpha) = \sum_{i=0}^m \alpha^i a_{m-i,n+m-i} s^{n+m-i}. \quad (55)$$

Observe that for every $\alpha > 0$, $\tilde{P}(s; \alpha)$ is evenly divisible by s^n . Dividing it by s^n , we define

$$\tilde{Q}(s; \alpha) := \sum_{i=0}^m \alpha^i a_{m-i, n+m-i} s^{m-i}, \quad (56)$$

and we note that

$$\tilde{P}(s; \alpha) = s^n \tilde{Q}(s; \alpha). \quad (57)$$

We make the observation that $\tilde{P}(s; \alpha)$ has the degree (in s) of $n + m$ hence it has $n + m$ roots; by (57), n of those roots are at $s = 0$, and the remaining m roots are the roots of $\tilde{Q}(s; \alpha)$. Finally, we define the m th-degree polynomial $Q(s)$ by setting $\alpha = 1$ in $\tilde{Q}(s; \alpha)$ (Eq. (56)); namely,

$$Q(s) := \tilde{Q}(s; 1) = \sum_{i=0}^m a_{m-i, n+m-i} s^{m-i}. \quad (58)$$

Observe that $Q(s)$ is independent of α , and its degree is m .

The following result establishes the α -stability of the system. Recall that Assumption 3 is implicit throughout the discussion.

Theorem 1. Consider the closed-loop system defined by Eq. (46). If the polynomials $P_0(s)$ and $Q(s)$ have all of their roots in the open Left-Half Plane (LHP), then the system is α -stable with respect to $\Omega := L^\infty(\mathcal{R}^m)$ and $\Gamma := \mathcal{R}^{n+m}$.

Before providing a proof, we offer a few comments on the theorem's statement and the system to which it pertains. The fact that the system is linear and time invariant ensures that $g(x, u)$ has a closed-form solution, as provided by Eq. (42). Consequently, a solution of the equation

$$r(t + T) = g(x(t), u(t))$$

is provided by the following formula,

$$u(t) = \left(CA^{-1}(e^{AT} - I)B \right)^{-1} \left(r(t + T) - Ce^{AT} x(t) \right). \quad (59)$$

In fact, for a given bounded exogenous reference signal $\{r(t)\}$, Eq. (59) corresponds to the limiting scenario, as $\alpha \rightarrow \infty$, of Eq. (45) as long as the terms $x(t)$ and $u(t)$ therein are uniformly bounded in (t, α) for $t \in [0, \infty)$ and large-enough α . This condition is closely related to, and follows from, the α -stability of the closed-loop system.

The first condition of Theorem 1, namely that all the roots of the polynomial $P_0(s)$ be in the open LHP, ensures the stability of the closed-loop system under the static feedback defined by Eq. (59). The second condition of Theorem 1, namely that all the roots of $Q(s)$ be in the LHP, ensures that the trajectories of the α -dependent systems with the dynamic feedback defined by (45) approach the trajectory of the system with the static feedback, as $\alpha \rightarrow \infty$. Now it may be practical to use the static feedback (defined by (59)) as long as all the roots of $P_0(s)$ are in the LHP, regardless of whether all the roots of $Q(s)$ also are in the LHP. However, this can lead to a discontinuous control signal $u(t)$ (see (59)) if $\{r(t)\}$ is discontinuous, which may be undesirable. The dynamic feedback defined by (45) may provide a suitable smooth approximation as long as both conditions of Theorem 1 are satisfied and hence the closed-loop system is α -stable.

The proof of Theorem 1 is based on the following two arguments: Under the assumptions stated in the theorem, for large-enough α , (i) the matrix Φ_α is Hurwitz, and (ii) $\{z(t)\}$ is bounded despite the fact that α is a multiplicative factor of some of the entries in the matrix Ψ_α (see (48)).

To prove the first argument we employ a root-locus technique for the eigenvalues of Φ_α as functions of $\alpha > 0$, in a nonstandard setting; accordingly, the functional dependence of $P(s; \alpha)$, whose roots are the eigenvalues of Φ_α , on α and s is via a two-dimensional polynomial. The proof proceeds as follows: First we show that bounded branches of the root locus must converge, as $\alpha \rightarrow \infty$, to the zeros of $P_0(s)$, and this follows standard root-locus arguments. Then we prove that the angles (arguments) of the unbounded branches of the root locus converge, as $\alpha \rightarrow \infty$, to angles of the roots of $Q(s)$, hence be in the LHP for large-enough α under the assumption that all of the roots of $Q(s)$ are in the LHP. As for the boundedness of $\|z(t)\|$ at large α , it will follow from the specific structures of the matrices Φ_α and Ψ_α .

Throughout the forthcoming discussion we denote a generic branch of the root locus of $P(s; \alpha)$ by $\{s(\alpha)\}_{\alpha \geq 0}$, or by $\{s(\alpha)\}$ for a simpler notation.

Lemma 2. If $\{s(\alpha)\}$ is bounded over $\alpha \in [0, \infty)$, then the limit $\lim_{\alpha \rightarrow \infty} s(\alpha)$ exists and it is a root of $P_0(s)$.

The proof is straightforward since $P_0(s)$ is the polynomial-coefficient of α^m in (50); please see ([18], Lemma 4.6).

Consider next the case where $\{s(\alpha)\}$ is unbounded. Let $A \subset [0, \infty)$ be an unbounded set such that

$$\lim_{\alpha \rightarrow \infty; \alpha \in A} |s(\alpha)| = \infty.$$

Lemma 3. There exist constants $c > 0$ and $C > c$ such that, as $\alpha \rightarrow \infty; \alpha \in A$,

$$c \leq \liminf \frac{|s(\alpha)|}{\alpha}, \quad \text{and} \quad \limsup \frac{|s(\alpha)|}{\alpha} \leq C. \quad (60)$$

Proof. Consider first the right inequality of Eq. (60). Let us argue by contradiction. If that inequality does not hold, there exists an unbounded set $A_1 \subset A$ such that, as $\alpha \rightarrow \infty, \alpha \in A_1$,

$$\frac{|s(\alpha)|}{\alpha} \rightarrow \infty. \quad (61)$$

By Eq. (50), $\forall \alpha \in A_1$,

$$\sum_{i=0}^m \alpha^i P_{m-i}(s(\alpha)) = 0.$$

Dividing this equation by $s(\alpha)^{m+n}$, we get that

$$\sum_{i=0}^m \left(\frac{\alpha}{s(\alpha)} \right)^i \frac{P_{m-i}(s(\alpha))}{s(\alpha)^{n+m-i}} = \sum_{i=1}^m \left(\frac{\alpha}{s(\alpha)} \right)^i \frac{P_{m-i}(s(\alpha))}{s(\alpha)^{n+m-i}} + \frac{P_m(s(\alpha))}{s(\alpha)^{m+n}} = 0. \quad (62)$$

But $\deg(P_{m-i}) = n + m - i$, hence, and by (51), as $\alpha \rightarrow \infty; \alpha \in A_1$,

$$\frac{P_{m-i}(s(\alpha))}{s(\alpha)^{n+m-i}} \rightarrow a_{m-i, n+m-i}$$

which is a finite-magnitude number. Therefore, and by (61),

$$\sum_{i=1}^m \left(\frac{\alpha}{s(\alpha)} \right)^i \times \frac{P_{m-i}(s(\alpha))}{s(\alpha)^{n+m-i}} \rightarrow 0$$

as $\alpha \rightarrow \infty; \alpha \in A_1$. Furthermore, $\deg(P_m) = n + m$, hence, and since the leading coefficient of P_m is 1,

$$\frac{P_m(s(\alpha))}{s(\alpha)^{m+n}} \rightarrow 1.$$

This contradicts (62) thereby ascertaining the right inequality of (60).

The left inequality of (60) is provable by similar arguments, hence a proof is omitted here but can be found in ([18], Lemma 4.7). \square

Consider the polynomial $P(s; \alpha)$ as defined by (50), and let $\{s(\alpha)\}$ be a branch of its root locus. Let us examine the derivative of $s(\alpha)$, for a given $\alpha > 0$, with respect to the coefficients of $P_{m-i}(s)$, for $i = 0, \dots, m$, as defined by Eq. (51). For this purpose we consider all but the leading coefficients, namely $a_{m-i, j}$, $j = 0, \dots, n + m - i - 1$. We denote these derivatives by $\frac{\partial s(\alpha)}{\partial a_{m-i, j}}$. For apparent reasons of notation, we will use ℓ and ν instead of i and j in the following discussion.

Lemma 4. There exist $r \geq 0$ and $L > 0$ such that, if $|s(\alpha)| \geq r$, then for every $\ell = 0, \dots, m$, and for every $\nu = 0, \dots, n + m - \ell - 1$,

$$\left| \frac{\partial s(\alpha)}{\partial a_{m-\ell, \nu}} \right| \leq L. \quad (63)$$

The proof is carried out by realizing that $P(s(\alpha); \alpha) = 0$, and taking derivatives with respect to $a_{m-\ell, \nu}$. The details can be found in ([18], Lemma 4.8). We remark that the assertion of Lemma 4 may not hold true for the case where $\nu = n + m - \ell$, namely for the leading coefficient of $P_{m-\ell}(s)$.

Recall the definition of $\tilde{P}(s; \alpha)$ which was made in Eq. (54). Similarly to the notation $s(\alpha)$ for a generic root of $P(s; \alpha)$, we denote by $\{\tilde{s}(\alpha)\}$ a generic branch of the root locus of $\tilde{P}(s; \alpha)$.

Lemma 5. There exist constants $r > 0$ and $K > 0$ such that, if $|s(\alpha)| \geq r$ for some $\alpha > 0$, then there exists $\tilde{s}(\alpha)$ such that

$$|\tilde{s}(\alpha) - s(\alpha)| < K. \quad (64)$$

Proof. The polynomials $P_{m-\ell}(s)$ and $\tilde{P}_{m-\ell}(s)$, $\ell = 0, \dots, m$, have the same respective leading coefficients, $a_{m-\ell, n+m-\ell}$. As for the other coefficients, those of $P_{m-\ell}(s)$ are $a_{m-\ell, \nu}$, $\nu = 0, \dots, n + m - \ell - 1$, and those of $\tilde{P}_{m-\ell}(s)$ are 0. Recall $L > 0$ in Eq. (63), and define $K := L \sum_{i=0}^m (n + m - i)$; the statement now follows from Lemma 4 and the mean-value theorem. \square

Fix $\alpha > 0$. It has been mentioned that, by Eq. (57), n of the roots of $\tilde{P}(s; \alpha)$ are at 0, and its remaining m roots are the roots of $\tilde{Q}(s; \alpha)$ as defined by (56). We next characterize the roots of $\tilde{Q}(s; \alpha)$.

Lemma 6. Let s be a root of the polynomial $Q(\cdot)$. Then for every $\alpha > 0$, αs is a root of the polynomial $\tilde{Q}(\cdot; \alpha)$.

Proof. By Eqs. (56) and (58), we see that for every complex variable s , and for every $\alpha > 0$,

$$\tilde{Q}(\alpha s; \alpha) = \alpha^m Q(s). \quad (65)$$

Therefore, if s is a root of $Q(\cdot)$, αs is a root of $\tilde{Q}(\cdot; \alpha)$. \square

Given a complex variable s , let $\angle s$ denote the angle (argument) of s with respect to the positive side of the horizontal axis. Thus, if $s = |s|e^{j\phi}$ according to its polar coordinates, then $\angle s = \phi$.

Lemma 7. Let s_i , $i = 1, \dots, m$, denote the roots of the polynomial $Q(s)$. Suppose that none of these roots is 0. For every unbounded branch of the root locus of $P(s; \alpha)$, denoted by $\{s(\alpha)\}$, there exists $i \in \{1, \dots, m\}$ such that,

$$\lim_{\alpha \rightarrow \infty} \angle s(\alpha) = \angle s_i. \quad (66)$$

Proof. By Lemma 6, m of the root-locus' branches of $\tilde{Q}(s; \alpha)$ are straight lines $\{\alpha s_i\}_{\alpha=0}^{\infty}$, $i = 1, \dots, m$. By Eq. (57), these are the unbounded root loci of $\tilde{P}(s; \alpha)$. Therefore, and by Lemma 5, if $\{s(\alpha)\}$ is unbounded, there exist $r > 0$, $K > 0$ and $i \in \{1, \dots, m\}$ such that, if $|s(\alpha)| > r$, then $|s(\alpha) - \alpha s_i| < K$. This implies Eq. (66) and completes the proof. \square

Proof of Theorem 1. Suppose that all of the roots of the polynomials $P_0(s)$ and $Q(s)$ are in the LHP. Then Lemma 2 and Lemma 7 imply that there exist $\sigma < 0$ and $\bar{\alpha} \geq 0$ such that $\forall \alpha \geq \bar{\alpha}$, all of the eigenvalues of the closed-loop system matrix Φ_α are to the left of the vertical line $(\sigma - j\infty, \sigma + j\infty)$ in the complex plane. This argument would be sufficient to prove the α -stability of the system were it not for the fact that the matrix Ψ_α is not a bounded function of α ; see (48). Nevertheless we next show that for every reference signal $\{r(t)\} \in \Omega \cap C$ and an initial condition $z_0 := z(0) \in \Gamma$, the state trajectory of Eq. (46) is bounded in α . This will complete the proof.

As a matter of notation, we say that a matrix is $O(\alpha^k)$ for an integer k (possibly nonpositive) if the highest power of α among all its entries is α^k . Recall Eq. (49), and note, that the first n rows of Φ_α do not contain α , and the last m rows contain α as a multiplicative factor. Therefore, by Cramer's rule, the first n columns of $(sI - \Phi_\alpha)^{-1}$ are $O(\alpha^0)$, and its last m columns are $O(\alpha^{-1})$. Denote by $\Phi_{1,\alpha}(s)$ and $\Phi_{2,\alpha}(s)$ the matrices comprised of the first n columns and last m columns of $(sI - \Phi_\alpha)^{-1}$, respectively. Then $\Phi_{1,\alpha}(s)$ is $O(\alpha^0)$, and $\Phi_{2,\alpha}(s)$ is $O(\alpha^{-1})$. As for Ψ_α , denote the matrix comprised of its last m rows by $\Psi_{2,\alpha}$. Then (by (48)), $\Psi_{2,\alpha}$ is $O(\alpha^1)$. Now the $r(t+T)$ -to- $z(t)$ (input-to-state) transfer function of the system defined by (46) is

$$(sI - \Phi_\alpha)^{-1} \Psi_\alpha = \begin{pmatrix} \Phi_{1,\alpha}(s) & \Phi_{2,\alpha}(s) \end{pmatrix} \begin{pmatrix} 0 \\ \Psi_{2,\alpha} \end{pmatrix} = \Phi_{2,\alpha}(s) \Psi_{2,\alpha}. \quad (67)$$

Since $\Phi_{2,\alpha}(s)$ is $O(\alpha^{-1})$ and $\Psi_{2,\alpha}$ is $O(\alpha^1)$, $(sI - \Phi_\alpha)^{-1} \Psi_{2,\alpha}$ is $O(\alpha^0)$, hence $\{z(t)\}$ is bounded. Consequently, and since Φ_α is Hurwitz, there exist $\xi < 0$ and $\tilde{\alpha} \geq 0$ such that, for every $\alpha \geq \tilde{\alpha}$, the real parts all the poles of the $r(t+T)$ -to- $z(t)$ transfer-function matrix are smaller than ξ . This, together with the fact that all of the eigenvalues of Φ_α are to the left of the line $(\sigma - j\infty, \sigma + j\infty)$, imply the α -stability of the closed-loop system with respect to $\Omega = L^\infty(\mathcal{R}^m)$ and any closed set $\Gamma = \mathcal{R}^{n+m}$. \square

Theorem 2. Consider the system defined by Eq. (41), with the controller defined by either (15), (22) or (39). Suppose that the target-reference process is exogenous. If the polynomials $P_0(s)$ and $Q(s)$ have all of their roots in the open LHP, then for every $\{r(t)\} \in C$ and $z_0 \in \mathcal{R}^{n+m}$,

$$\lim_{\alpha \rightarrow \infty} \limsup_{t \rightarrow \infty} \|r(t) - \hat{y}(t)\| = 0. \quad (68)$$

Proof. Follows from Proposition 3 and Theorem 1. \square

Remark 2. A few words must be said about the relationships between α -stability of linear systems and the controllability, observability, and minimum phase of their plant subsystems. If the plant subsystem is not completely observable and all of its unobservable modes correspond to LHP eigenvalues of A , then $x(t)$ in the control equations can be replaced by the state variable of a suitable Luenberger observer without changing the result of Theorem 2. As for controllability, by Definition 1, α -stability implies the boundedness of $\{x(t)\}$, and in that case unreachable modes of the plant cannot be associated with RHP eigenvalues of A . Finally, α -stability of the closed-loop system does not require the plant to be a minimum-phase system, as the following example demonstrates.

Example. Let

$$A = \begin{pmatrix} 2 & 1 \\ -1 & -1 \end{pmatrix}, \quad B = \begin{pmatrix} 0 \\ 1 \end{pmatrix}, \quad C = (-10 \ 1),$$

and $T = 0.25$ s. The plant transfer function is

$$G(s) = \frac{s - 12}{s^2 - s - 1},$$

which is neither stable nor of a minimum phase. Next, $P(s; \alpha) = (s^3 - s^2 - s) + \alpha(s^2 + 16.19s + 97.18)$. Therefore $P_0 = s^2 + 16.19s + 97.18$ and $P_1(s) = s^3 - s^2 - s$, implying that $Q(s) = s + 1$. Both $Q(s)$ and $P_0(s)$ have all of their roots in the LHP, hence the system is α -stable.

5 | SIMULATION EXPERIMENTS

This section presents simulation results for two problems concerning, respectively, an inverted pendulum and a platoon of autonomous vehicles. For the inverted pendulum we use the controller defined by Eq. (22). As for the platoon system, $\{r(t+T)\}$ is a controlled (endogenous) process, and to avoid a real-time computation of $\dot{r}(t+T)$ we choose the controller based on Eq. (15).

5.1 | Inverted pendulum

Ref. [15] concerns the control of an inverted pendulum by the torque directly applied to the base of its pole. Here we consider the more-challenging problem of a pole on a cart, controlled by the horizontal force on the cart.

The cart can move in the two directions of a given line, parameterized by $z \in R$. Let θ denote the angle of the pendulum from its pivot on the cart to the left of the upward-vertical direction. Thus, if the pendulum is pointed upwards then $\theta = 0$, and if it points sideways along the z axis in the positive direction then $\theta = -\pi/2$ rads. Let M and m denote the masses of the cart and pendulum, respectively, and let ℓ be the distance from the cart to the pendulum's center of mass. Let F be the force applied to the cart in the positive direction of the z axis.

Generally this system is four-dimensional with input F and state variable $(z, \dot{z}, \theta, \dot{\theta})$. Our interest is in controlling θ which therefore is taken as the system's output. A simpler, second-order representation of the pendulum's motion can be obtained by making the following two assumptions: 1). The pendulum consists of a weightless rod and a point mass at its end. 2). There is no friction in the movement of the cart or the pendulum. In this case, the dynamic equation of the pendulum's motion becomes

$$(M\ell + m\ell \sin^2 \theta)\ddot{\theta} + m\ell \dot{\theta}^2(\sin \theta)(\cos \theta) - (M + m)g \sin \theta = F \cos \theta; \quad (69)$$

see [21]. This equation provides a state-space representation of the system where the state variable is $x = (\theta, \dot{\theta})^\top$, the input is $u = F$, and the output is $y = \theta$. We chose the following parameters for the simulation: $M = 1$ kg, $m = 0.2$ kg, $\ell = 2$ m, and $g = 9.81$ m/s². The simulation starts at the initial state $x(0) = (\frac{\pi}{6}, 0)^\top$, and it solves the state equation in a specified horizon $t \in [0, t_f]$ by the forward Euler method with the step-size $dt = 0.01$ s. We apply the control algorithm defined by Eq. (22) with the prediction horizon $T = 0.2$ s, and it computes the predicted state trajectory (Eq. (17)) by the forward-Euler method with the step-size $\Delta t = 0.01T$. The initial condition for the controller equation (22) is $u(0) = 0$.

The target trajectory for the tracking-control experiment is $r(t) = -\frac{\pi}{6} + \frac{\pi}{3} \sin t$, which oscillates between the angles of 30° and -90°. At -90° the pendulum points at the horizontal direction along the positive z -axis, and this can be problematic because it is physically impossible to balance the pendulum at this angle. However, in the present experiment $r(t)$ just touches the horizontal direction and then immediately retreats therefrom. The time-horizon for the simulation is $t_f = 25$ s.

For the controller's equation (22) we first took $\alpha = 1$, and noted convergence of $\theta(t)$ to $r(t)$ in about 2 seconds. To speed up the convergence we increased the controller's gain to $\alpha = 35$, and the results are depicted in Figures 2-3. Figure 2 shows the graphs of $\theta(t)$ in blue and the reference $r(t)$ in red. The two graphs appear to coalesce for the first time at about $t = 1$ s, and remain close to each other thereafter except for slight differences when $r(t) \sim -\frac{\pi}{2}$ rads (about -1.57 in the graph). These slightly-larger errors are not surprising because at such points the pendulum is horizontal. The maximum error, $|r(t) - \theta(t)|$, for $t \geq 1$ was measured from the graphs at 0.022 radians, or 1.2605 degrees. The graph of the control signal $u(t)$ is depicted in Figure 3, and we notice large peaks at the points where $r(t) = -\frac{\pi}{2}$. This is expected in light of the above remarks concerning a control of the pendulum at the horizontal angle. To verify that the discrepancies between $r(t)$ and $\theta(t)$ and the large control input are largely due to the proximity of $\theta(t)$ to $-\frac{\pi}{2}$, we attenuated the sinusoidal part of $r(t)$ by a factor of 0.8, corresponding to oscillations between the

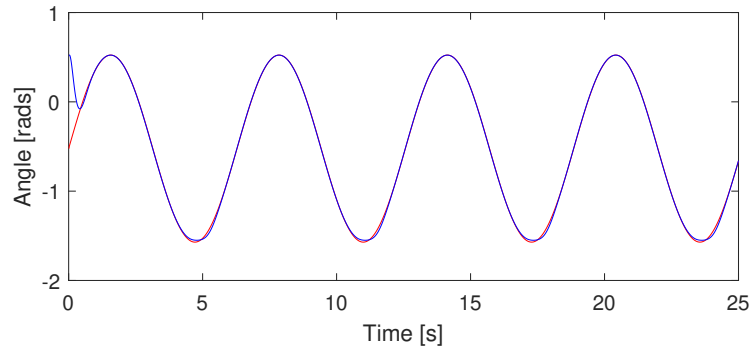


FIGURE 2 Inverted pendulum: θ and r vs. t

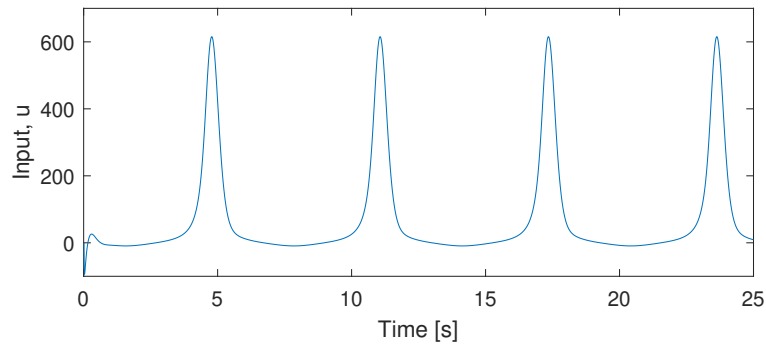


FIGURE 3 Inverted pendulum: u vs. t

angles of 18° and -78° . The results are not presented here but can be seen in ([18, 22]); they exhibit considerably-less distortion, and a peak control input of about 60 which is roughly 10% of the peak control value (about 600) that is indicated in Figure 3.²

5.2 | Platoon of autonomous vehicles

The simulation experiment described in this subsection concerns the planar motion of a platoon, controlled to follow a given path in the (z_1, z_2) plane. The platoon consists of four agents (vehicles), denoted by A_i , $i = 1, 2, 3, 4$, in the order of their movement. A_1 is the leading vehicle, and A_i follows A_{i-1} , $i = 2, 3, 4$. A_1 is provided with an exogenous reference trajectory (path) to track, $\{r_1(t)\}$, and for $i = 2, 3, 4$, A_i attempts to follow A_{i-1} at a prescribed distance (arclength) of d m on the path. Whereas the target reference for each agent remains on the path $\{r_1(t)\}$, the agent itself can veer off the path while pursuing its target. In this way the agents' motions are two-dimensional and not confined to a prescribed one-dimensional curve. We assume that each agent

²Ref. [22] concerns a neural-network approximation of the output predictor thereby rendering the controller model-free. It failed to converge for the sinusoidal span of the target reference considered here, probably due to its extreme values at $-\frac{\pi}{2}$. However, it worked well for the reduced span of the sinusoid by 80% as described above.

controls its own motion: $u_1(t)$ depends of $r_1(t)$, while for $i = 2, 3, 4$, $u_i(t)$ is computed by the position and velocity of A_{i-1} , which are assumed to be measured by A_i or transmitted to it by A_{i-1} .

The motion-dynamics of the vehicles follow the bicycle model, a sixth-order nonlinear system that has been extensively used in the design and analysis of motion control for autonomous vehicles; see, e.g., [23] and references therein. In [17] we demonstrated the tracking technique on a single vehicle having such a model, while here we consider a platoon and apply the tracking-control to a path with a higher curvature.

The state space of the considered bicycle model consists of the six-tuple $x = (z_1, z_2, v_\ell, v_n, \psi, \dot{\psi})^\top$, where z_1 and z_2 are the planer position-coordinates of the center of gravity of the vehicle, v_ℓ and v_n are the longitudinal and lateral velocities, ψ is the heading of the vehicle and $\dot{\psi}$ is its angular velocity. The input, $u = (a_\ell, \delta_f)^\top$, consists of the longitudinal acceleration and steering angle of the front wheel, respectively, and the output is the position of the center of gravity of the vehicle, namely $y = (z_1, z_2)^\top$.

The dynamic equations of the vehicles are given by the following equations (see [24]),

$$\dot{z}_1 = v_\ell \cos \psi - v_n \sin \psi \quad (70)$$

$$\dot{z}_2 = v_\ell \sin \psi + v_n \cos \psi \quad (71)$$

$$\dot{v}_\ell = \dot{\psi} v_n + a_\ell \quad (72)$$

$$\dot{v}_n = -\dot{\psi} v_\ell + 2(F_{c,f} \cos \delta_f + F_{c,r})/m \quad (73)$$

$$\dot{\psi} = 2(l_f F_{c,f} \cos \delta_f - l_r F_{c,r})/I_z, \quad (74)$$

where m is the mass of the vehicle, l_f and l_r are the front and back axles' distances from the vehicle's center of mass, I_z is the yaw moment of inertia, and $F_{c,f}$ and $F_{c,r}$ are the lateral forces on the front and rear wheels. These forces are approximated by the following equations,

$$F_{c,f} = C_{\alpha,f} (\delta_f - \tan^{-1}((v_n + l_f \dot{\psi})/v_\ell)) \quad (75)$$

$$F_{c,r} = -C_{\alpha,r} \tan^{-1}((v_n - l_r \dot{\psi})/v_\ell), \quad (76)$$

where $C_{\alpha,f}$ and $C_{\alpha,r}$ are the cornering stiffness of the front and rear tires, respectively.

In the simulation we used the following model-parameters as in [25], Volvo V70 model, except for I_z (not provided there) which has been estimated by data from cars of similar weight and dimensions: $m = 1,700\text{kg}$, $l_r = 1.5\text{m}$, $l_f = 1.5\text{m}$, $I_z = 2,500\text{kg} \cdot \text{m}^2$, and $C_{\alpha,f} = C_{\alpha,r} = 29,963.5\text{N/rad}$. As for the problem, controller and simulation parameters, the desired inter-agent distance is $d = 10\text{m}$, the simulation horizon is $t_f = 38\text{s}$, and the discretization step size for the simulation is $dt = 0.01$ secs. The controller prediction horizon is set to $T = 0.5\text{s}$, and the discretization time step for the predictor is $\Delta T = 0.001T$. $\alpha = 100$ for all the vehicles. The target trajectory $\{r_1(t)\}$ is indicated by the curve in Figure 4, and its acceleration along the path is indicated by the blue graph in Figure 5. Its initial speed is $\dot{r}_1(0) = 0$, and its largest speed, obtained at $t \in [10, 15]$ and again at $t \in [25, 30]$, is 20m/s . At the point of largest curvature, when z_2 attains its maximum (see Figure 4), its speed is 8.66m/s . The four vehicles start at rest at the point $r_1(0)$, and the initial condition of their controller is $u(0) = (2, 0)^\top$.

Simulation results with the controller defined by Eq. (15) are shown in Figures 4-7. Figure 4 depicts the trajectories of the reference target and vehicles' motions from left to right in the (z_1, z_2) plane. It is hard to distinguish between the various trajectories in the figure due to its large scale of the planer, (z_1, z_2) coordinates. Both coordinates are of the same scale, hence the curvature can be seen to be quite large at the point of maximum z_2 . Figure 5 depicts the longitudinal accelerations of the target reference and vehicles' trajectories. While apparently making for an uncomfortable ride, they closely track the acceleration of the target path $\{r_1(t)\}$ with a notable deviation corresponding to its region of largest curvature.

Figure 6 shows the graphs of the lateral (normal) errors of the vehicles' centers of gravity from the target trajectory $\{r_1(t)\}$, and we note that the relatively large error-spurts correspond to the higher accelerations and larger curvatures indicated in Figure 5 and Figure 4, respectively. Furthermore, as expected, the errors of later vehicles in the platoon tend to be larger than those of earlier ones. The maximum lateral error, obtained for A_4 , is about 38cm .

Graphs of a measure of the inter-agent distances are shown in Figure 7. The objective of the control law is to have the vehicles approach the path $\{r_1(t)\}$ at the inter-agent distance of 10m , and since the distance is measured by the arclength, there is no corresponding natural measure of distance when two vehicles are off the path. For this case we define the approximate-measure of inter-agent distance as the arclength between the closest points to the vehicles on the curve $\{r_1(t)\}$ plus the Euclidean distances between the vehicles' centers of gravity and those points. It is this measure of distance that is depicted in Figure 7. Now Figure 6 and Figure 7 suggest that this measure is reasonable because it converges to the target level of 10m except in regions of large lateral errors.

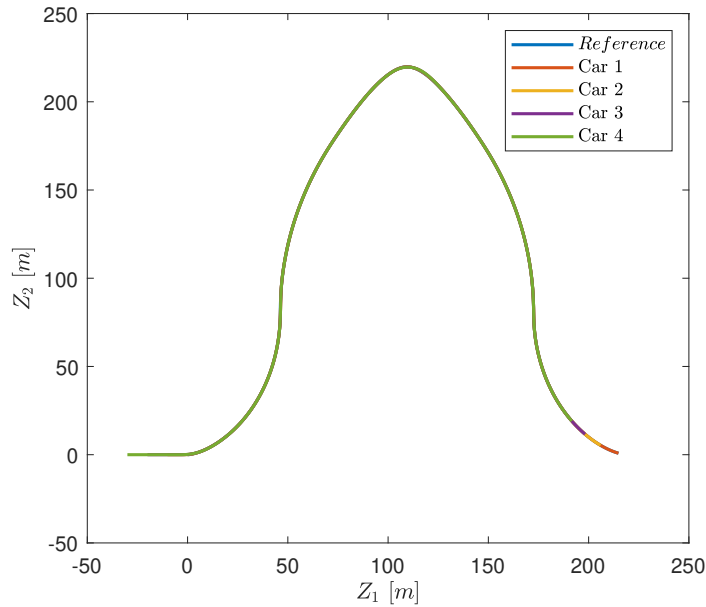


FIGURE 4 Platoon: target trajectory in the z-plane

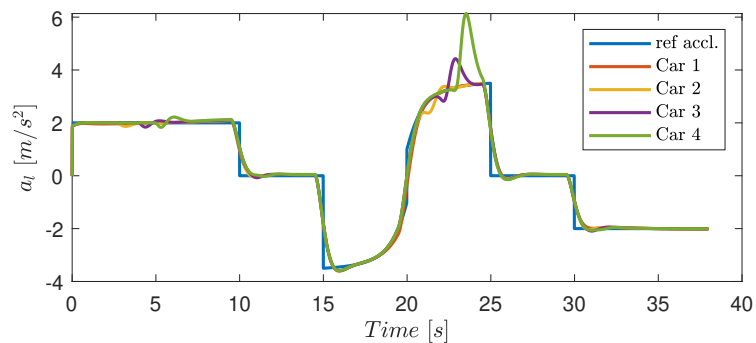


FIGURE 5 Platoon: Reference-path and vehicle accelerations

6 | EXPERIMENTAL RESULTS

This section describes results of laboratory experiments in which a platoon of four mobile robots (agents) attempts to maintain a given inter-agent distance. Denote the agents by A_i , $i = 1, \dots, 4$, according to their order in the platoon. A_1 is assigned its target trajectory, $\{r_1(t)\}$, by an exogenous source, and for every $i = 2, 3, 4$, A_i has to keep a given Euclidean distance from A_{i-1} . The present system is different from the one considered in Subsection 5.2 in several ways including the following three: (i) The experimental setting is a laboratory vs. simulation, (ii) the respective dynamic models are different, and (iii) A_i , $i = 2, 3, 4$, only have to maintain the given inter-agent distance from A_{i-1} but not follow its trajectory on a prescribed curve.

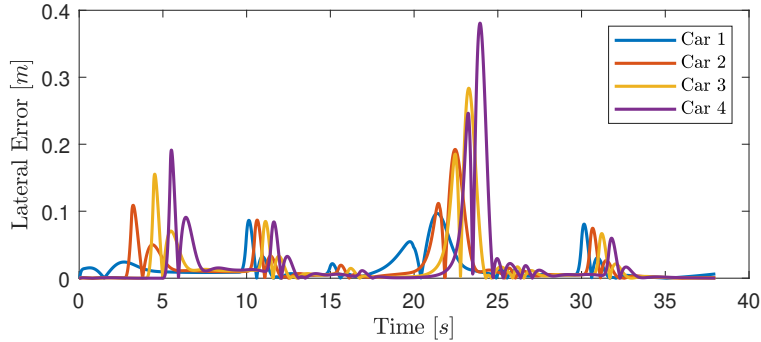


FIGURE 6 Platoon: lateral errors vs. time

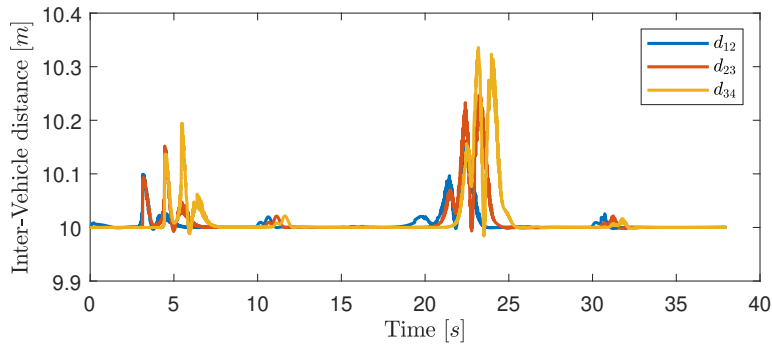


FIGURE 7 Platoon: inter-agent distances

The experiments were conducted in the Robotarium, a remotely-accessible testing facility for motion control of networks of mobile robots located at the Georgia Tech campus ([26]). The robots in the Robotarium are differential-drive robots, approximately 15cm in diameter, which were designed and assembled in-house. Their motion is modelled by unicycle dynamics having the following form,

$$\begin{pmatrix} \dot{z}_1(t) \\ \dot{z}_2(t) \\ \dot{\psi}(t) \end{pmatrix} = \begin{pmatrix} \cos \psi(t) & 0 \\ \sin \psi(t) & 0 \\ 0 & 1 \end{pmatrix} \begin{pmatrix} v(t) \\ \omega(t) \end{pmatrix}, \quad (77)$$

where $z := (z_1, z_2)^\top \in \mathcal{R}^2$ is the center of gravity of a robot, and ψ is its heading. The control input is $u := (v, \omega)^\top$, where v is the longitudinal velocity and ω is the angular velocity. The output of the system is $y(t) := z(t) = (z_1(t), z_2(t))^\top$. The term $g(x(t), u(t))$ has the following analytic form,

$$g(x(t), u(t)) = \begin{pmatrix} z_1(t) \\ z_2(t) \end{pmatrix} + \frac{v(t)}{\omega(t)} \begin{pmatrix} \sin(\psi(t) + \omega(t)T) - \sin(\psi(t)) \\ -\cos(\psi(t) + \omega(t)T) + \cos(\psi(t)) \end{pmatrix}; \quad (78)$$

if $\omega(t) = 0$, L'Hopital's rule yields

$$g(x(t), u(t)) = T v(t) \begin{pmatrix} \cos(\psi(t)) \\ \sin(\psi(t)) \end{pmatrix}. \quad (79)$$

We mention that in [17] we considered a transformation of the unicycle model in such a way that its motion dynamics consist of a single two-dimensional integrator. In contrast, here we consider the fully-dynamical system defined by (77), and a different tracking objective.

The predicted target-point $r_i(t + T)$ is defined for the agent A_i according to the following heuristic. For $i = 1$, $\{r_1(t)\}$ is an exogenous process assumed to be known in advance, and hence $r_1(t + T)$ can be used in the computations for A_1 at time t . For $i = 2, 3, 4$, the definition and computation of $r_i(t + T)$ are recursive, as follows. Let $d > 0$ be the target distance between the agents. $r_i(t + T)$ is defined as the point on the line segment connecting the position of A_i at time t and the predicted position of A_{i-1} at time $t + T$, located d m from the predicted position of A_{i-1} . For a justification of this choice please see [18], including the fact that if A_1 moves in a straight line then subsequent agents will converge to that line behind each other.

We conducted experiments with the controller defined by Eqs. (15) and (39), respectively; $\alpha = 45$ and $T = 0.25$ s. The former controller gave slightly better results, hence we present them below. The exogenous target curve, $\{r_1(t)\}$, is an ellipse defined by $r_1(t) = (1.1 \sin(0.06t), 0.7 \cos(0.06t))^T$, and the target inter-robot distance is $d = 0.25$ m. The results are depicted in Figures 8-9.

Figure 8 depicts the inter-robot distances vs. t , and we note convergence towards the target distance of 0.25m. Figure 9 depicts the graph of the tracking error $\|y_i(t) - r_i(t)\|$ versus time, and we discern rapid convergence towards 0 for all four robots. Explicit views of the robots' motion trajectories can be seen in the video clip contained in [27], and in the stills captured during the experiment, depicted in ([18], Figure 10). All of this suggest a convergence of the tracking-control algorithm.

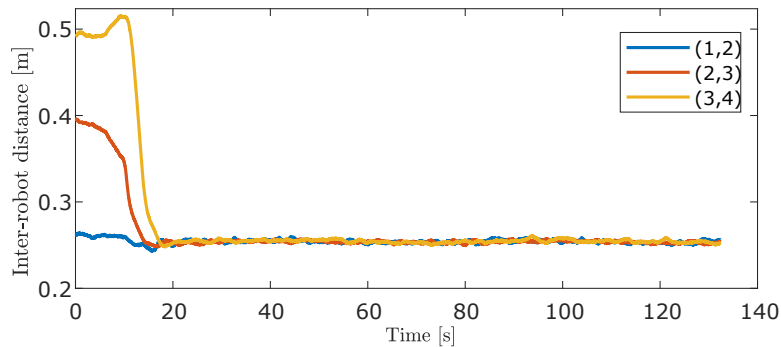


FIGURE 8 Experiment: inter-robot distances vs. time

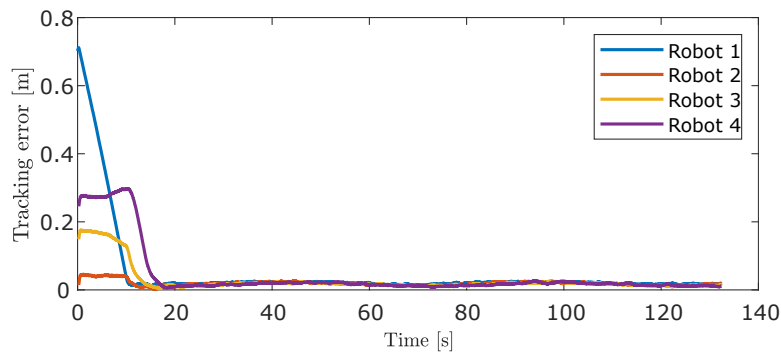


FIGURE 9 Experiment: tracking error vs. time

7 | CONCLUSIONS

This paper presents a tracking-control technique based on a fluid-flow version of the Newton-Raphson method, output prediction and controller speedup. The controller can be simple to compute and may have fast tracking convergence. The paper defines a suitable notion of local stability, and proves it to be sufficient for tracking. Furthermore, it proves a global stability for a class of linear systems. Simulation and laboratory experiments are presented in support of the theoretical results.

References

- [1] A. Isidori and C.I. Byrnes. “Output regulation of nonlinear systems”. In: *IEEE Transactions on Automatic Control* 35 (1990), pp. 131–140.
- [2] H.K. Khalil. “On the design of robust servomechanisms for minimum phase nonlinear systems”. In: *Proc. 37th IEEE Conference on Decision and Control*, Tampa, FL. 1998, pp. 3075–3080.
- [3] J.B. Rawlings, D.Q. Mayne, and M.M. Diehl. *Model Predictive Control: Theory, Computation, and Design, 2nd Edition*. Nob Hill, LLC, 2017.
- [4] S. Shivam et al. “A Predictive Deep Learning Approach to Output Regulation: The Case of Collaborative Pursuit Evasion”. In: *Proc. 58th IEEE Conference on Decision and Control*, Nice, France, December 11–13. 2019.
- [5] K. Arrow, L. Hurwicz, and H. Uzawa. *Studies in Linear and Nonlinear Programming*. Stanford, California: Stanford University Press, 1958.
- [6] R.W. Brockett. “Dynamical systems that sort lists, diagonalize matrices, and solve linear programming problems”. In: *Linear Algebra and Its Applications* 146 (1991), pp. 79–91.
- [7] U. Helmke and J.B. Moore. *Optimization and Dynamical Systems*. Springer, isbn 0387198571, 1994.
- [8] J.D. Lee et al. “Gradient Descent Only Converges to Minimizers”. In: *J. Machine Learning Research* 49 (2016), pp. 1–21.
- [9] N.K. Dhingra, S.Z. Khong, and M.R. Jovanović. “The proximal augmented Lagrangian method for nonsmooth composite optimization”. In: *IEEE Transactions on Automatic Control* 64.7 (2019), pp. 2861–2868.
- [10] W. Su. “Traffic Engineering and Time-Varying Convex Optimization”. PhD thesis. The Pennsylvania State University, 2009.
- [11] S. Rahili and W. Ren. “Distributed continuous-time convex optimization with time-varying cost functions”. In: *IEEE Transactions Automatic Control* 62.4 (2017), pp. 1590–1605.
- [12] N.K. Dhingra, S.Z. Khong, and M.R. Jovanović. “A second order primal-dual method for nonsmooth convex composite optimization”. In: *IEEE Transactions on Automatic Control* (2021). doi:10.1109/TAC.2021.3115449; also arXiv:1709.01610.
- [13] E.D. Sontag. “Smooth Stabilization Implies Coprime Factorization”. In: *IEEE Trans. Automatic Control* 34.4 (1989), pp. 435–443.
- [14] S. Kolathaya et al. “Input to State Stabilizing Control Lyapunov Functions for Robust Bipedal Robotic Locomotion”. In: *American Control Conference*, Milwaukee, Wisconsin, June 27–29. 2018.
- [15] Y. Wardi et al. “Performance Regulation and Tracking via Lookahead Simulation: Preliminary Results and Validation”. In: *56th IEEE Conf. on Decision and Control*, Melbourne, Australia, December 12–15. 2017.
- [16] Y. Wardi, C. Seatzu, and M. Egerstedt. “Tracking Control via Variable-gain Integrator and Lookahead Simulation: Application to Leader-follower Multiagent Networks”. In: *6th IFAC Conf. on Analysis and Design of Hybrid Systems (ADHS’18)*, Oxford, UK, July 11–13. 2018.
- [17] S. Shivam et al. “Tracking Control by the Newton-Raphson Flow: Applications to Autonomous Vehicles”. In: *Proc. 2019 European Control Conference (ECC 2019)*, Napoli, Italy, June 25–28. 2019.
- [18] Y. Wardi et al. “Tracking Control by the Newton-Raphson Method with Output Prediction and Controller Speedup”. In: *arxiv*, <http://arxiv.org/abs/1910.00693>. 2019.
- [19] A. Kanellopoulos, K. Vamvoudakis, and Y. Wardi. “Predictive Learning via Lookahead Simulation”. In: *Proc. AIAA SciTech Forum*, San Diego, California, June 7–11. 2019.
- [20] E. Polak. *Optimization Algorithms and Consistent Approximations*. Springer-Verlag, New York, New York, 1997.
- [21] Wikipedia. In: https://en.wikipedia.org/wiki/Inverted_pendulum. 2010.
- [22] K. Niu et al. “A Model-free Tracking Controller Based on the Newton-Raphson Method and Feedforward Neural Networks”. In: *Proc. American Control Conference (ACC)*, Atlanta, Georgia, June 8–10, forthcoming. 2022.

- [23] M.G. Plessen et al. “Spatial-Based Predictive Control and Geometric Corridor Planning for Adaptive Cruise Control Coupled with Obstacle Avoidance”. In: *IEEE Transactions Control Systems Technology* 26.4 (2018), pp. 38–50.
- [24] J. Kong et al. “Kinematic and Dynamic Vehicle Models for Autonomous Driving Control Design”. In: *Proc. IEEE Intelligent Vehicles Symposium (IV)*. 2015.
- [25] Mathworks.com. In: <https://www.mathworks.com/help/ident/examples/modeling-a-vehicle-dynamics-system.html>. 2019.
- [26] D. Pickem et al. “The Robotarium: A Remotely Accessible Swarm Robotics Research Testbed.” In: *IEEE Int. Conf. Robot. Autom.* May 2017.
- [27] I. Buckley. In: <https://youtu.be/4CSlgrxcu8>. 2019.

